Fish and Shellfish Immunology 89 (2019) 458–467

Contents lists available at ScienceDirect

Fish and Shellfish Immunology

journal homepage: www.elsevier.com/locate/fsi

Full length article

Proteomic analysis and white spot syndrome virus interaction of mud crab *(Scylla olivacea)* revealed responsive roles of the hemocytes

Phattara-orn Havanapan[a], Seksan Mangkalanan[a,b], Nuanwan Phungthanom[a], Chartchai Krittanai[a,*]

[a] Institute of Molecular Biosciences, Mahidol University, Salaya Campus, Nakhon Pathom, Thailand
[b] Department of Applied Biology, Faculty of Sciences and Liberal Arts, Rajamangala University of Technology Isan, Nakhon Ratchasima, Thailand

ARTICLE INFO

Keywords:
White spot syndrome virus
S. olivacea
Mud crab
Hemocyte
Crustacean
Proteomic
Apoptosis

ABSTRACT

White spot disease (WSD) is a highly virulent viral disease in shrimps. Clinical signs and high mortality of WSD is generally observed after a few days of infection by White Spot Syndrome virus (WSSV). Mud crabs are the major carrier and persistent host for the WSSV. However, an elucidation of viral interaction and persistent mode of WSSV infection in mud crab is still limited. We investigated the defensive role of mud crab (*Scylla olivacea)* hemocytes against WSSV infection by using comparative proteomic analysis coupled with electrospray ionization liquid chromatography tandem mass spectrometry (ESI-LC/MS/MS). The proteomic maps of expressed proteins obtained from WSSV infected hemocytes revealed differential proteins related to various biological functions, including immune response, anti-apoptosis, endocytosis, phosphorylation signaling, stress response, oxygen transport, molting, metabolism, and biosynthesis. Four distinctive cell types of crab hemocytes: hyaline cells (HC), small granular cells (SGC), large granular cells (LGC) and mixed granular cells (MGC) were found susceptible to WSSV. However, immunohistochemistry analysis demonstrated a complete replication of WSSV only in SGC and LGC. WSSV induced apoptosis was also observed in HC, SGC and MGC except for LGC. These results suggested that HC and MGC may undergo apoptosis prior to a complete assembly of virion, while SGC is more susceptible showing higher amplification and releasing of virion. In contrast, WSSV may inhibit apoptosis in infected LGC to stay in latency. This present finding provides an insight for the responsive roles of crustacean hemocyte cells involved in molecular interaction and defense mechanism against WSSV.

1. Introduction

White spot syndrome virus (WSSV) is the causative agent of white spot disease (WSD), causing up to 100% mortality rate of shrimp in a few days [42]. WSSV outbreaks became the most serious problem for shrimp culture farming and leading to enormous economic loss in Thailand since 1996. The infected shrimps showed many clear white spots on exoskeleton and epidermis of the carapaces. WSSV is the rod-shaped close circular double stranded DNA virus classified in the genus *Whispovirus*, and Nimaviridae family [24]. To date, at least 40 structural proteins were identified [7,49,50]. Two major envelope proteins, VP26 and VP28, play a critical role in the systematic infection process and act as the attachment protein for shrimp cell binding and cytoplasm entry [63]. Recent study revealed that the interaction between VP26 and WSSV-binding protein inhibits an invasion of WSSV into host cells [64].

WSSV has a broad host range. Several host species such as penaeid shrimps, crabs and lobsters were found susceptible to WSSV infection [15,35]. The susceptible hosts can be classified into symptomatic, resistant and carrier hosts [8,12,35]. Mud crabs of *Scylla* spp. has been reported as the carrier host for WSSV. The clinical sign of WSD was not observed in an infected crab despite WSSV was detected by PCR and histological examination for a long survival period [43]. In contrast the symptomatic host such as penaeid shrimps usually die within a short time at the same dose of WSSV infection [35].

The defensive mechanism of crustacean depends on innate immunity [39]. Hemocytes, the responsive factor, demonstrated different defensive patterns depending on host types and infection methods. Many crustaceans' hemocytes were involved in phagocytosis, melanization, cytotoxicity and cell to cell communication during bacteria and fungi invasion [18]. Based on specific morphology and granularity, hemocytes of *Scylla olivacea* mud crab have been characterized recently as hyaline cell (HC), small granular cell (SGC), large granular cell (LGC) and mixed granular cell (MGC) [30]. Other classification by an abundance of granules was also reported as granulocyte, semi-granulocyte

* Corresponding author. Institute of Molecular Biosciences, Mahidol University, Salaya Campus, Nakhon Pathom, 73170, Thailand.
E-mail address: chartchai.kri@mahidol.ac.th (C. Krittanai).

https://doi.org/10.1016/j.fsi.2019.03.070
Received 28 December 2018; Received in revised form 27 March 2019; Accepted 28 March 2019
Available online 05 April 2019

and hyalinocyte [66]. A significant decrease of total hemocyte count were observed at 48 hpi in WSSV infected *Scylla Olivacea* mud crab and *Penaeus monodon* shrimp [30,51]. However, only the WSSV-infected *P. monodon* proceeded to moribund state. An interaction between WSSV and different cell types of hemocytes was studied in other crustaceans such as crayfish and banana shrimp [17,55]. The semi-granular cells showed greater viral interaction than that of granular cells. In contrast, hyaline cells showed very little interaction with the virus. However the molecular mechanism of mud crab hemocyte cell in response to WSSV infection remains uncharacterized.

Proteomic analysis has been applied to identify differential protein expression in WSSV-infected shrimp cells such as lymphoid organ of *P. vannamei*, epithelial cell of *P. monodon* and hepatopancreas of *P. chinensis* shrimps [5,53,59]. Recently, differential proteins in *S. paramamosain* crab have been investigated during *Vibrio alginolyticus* and WSSV infection [47]. Since the crustacean defense mechanism is restricted mainly to the hemocyte cells, this present study aims to uncover the functional and responsive roles of *S. olivacea* hemocytes during the persistent infection with WSSV. The results from identified differential proteins along with characterization of WSSV and hemocyte interaction may provide an insight for the detail mechanism of crab defense system. The acquired knowledge could be beneficial to the control and prevention of viral diseases for a sustainable aquaculture industry.

2. Materials and methods

2.1. WSSV infection of mud crab and hemocyte isolation

WSSV was obtained from the Center of Excellence in Shrimp Molecular Biology and Biotechnology (Centex Shrimp), Mahidol University. WSSV stock in serum was quantified by real time PCR as previously described [45]. Healthy male mud crab (*S. olivacea*) with 12–15 cm in length and average weight of 350 g were obtained from local market in Nakhon Pathom, Thailand. Each individual crabs were acclimatized in a plastic cage submerged in artificial sea water with 30 ppt salinity. They were fed with sea bass and the artificial sea water was changed daily. The crabs sample were divided into control (n = 12) and WSSV-infected group (n = 12). For an infected group, each crab was injected with WSSV at 10^5copy/g. The control group was injected with normal saline (0.9% NaCl). After one day post infection (dpi), crab hemolymph was collected from the hemocoel using 21G needle, and mixed with an equal volume of anticoagulant AC-1 solution (containing 30 mM citric acid, 10 mM EDTA, 0.45 M NaCl, 0.1 M glucose and 26 mM sodium citrate; pH 4.6) and then immediately kept on ice to prevent clotting. Hemocytes were harvested by centrifugation at 800*g* for 10 min at 4 °C. After discarding of plasma, the packed hemocytes were washed twice with AC-1 solution and stored at −20 °C until used.

2.2. Fractionation and extraction of hemocytic proteins

To reduce the complexity of 2-D PAGE analysis, protein samples were extracted from crab hemocyte and fractionated before applied to the two dimensional (2-D) gel electrophoresis. The collected hemocytes were initially lysed by cold buffer [3]. The mixture was centrifuged at 600*g* for 5 min. The supernatant were collected and transferred to the new tubes before centrifugation at 6,000*g* and subsequently at 20,200*g* for 20 min. The three fractionated pellets and one supernatant fraction were collected and re-suspended in RIPA buffer (0.1% SDS, 0.5% sodium deoxycholate, 1% triton X-100, 50 mM tris-HCl, pH 7.4, 150 mM NaCl, 1X protease inhibitor cocktail). The proteins from each fraction were precipitated by chloroform-methanol method. Briefly, 150 µl of protein solubilized in RIPA buffer was incubated with 600 µl methanol, 150 µl chloroform and 450 µl deionized water. The mixture was centrifuged at 14,000*g* for 10 min at 4 °C. The protein pellet was rinsed with 1 ml methanol and then air dried. The protein pellets was rehydrated in lysis solution containing 8 M urea, 2 M thiourea, 4% CHAPS, 0.1% triton X-100, 50 mM dithiothreitol, 1X protease inhibitor cocktails [Roche]. The mixture was incubated on ice for 10 min and in ultrasonic bath for 30 min and centrifuged at 14,000*g*, 4 °C for 5 min. The supernatant was kept at −20 °C until used. Protein concentration was determined by Bradford assay using bovine serum albumin (BSA) as a standard.

2.3. 2-D PAGE and protein identification by LC/MS/MS

Two dimensional polyacrylamide gel electrophoresis of the hemocytic protein fraction was conducted by pooling an equal protein samples from four individual crabs on each gel. A triplicated 2-D gels (12 individual crabs) were performed for control and WSSV-infected groups. Pooled protein sample of 400 µl from each fraction was separated on immobilized pH gradient strip [GE Healthcare] with 13 cm in length, nonlinear pH 3–10. First dimensional separation was conducted on Ettan IPGphor II electrode platform [GE Healthcare] using an optimized focusing profile of an increasing voltage (up to 8000 V) to reach 20,000 V-hrs. The focused gel strips were incubated in equilibration buffer (75 mM Tris–Cl, pH 8.8, 6 M urea, 2% SDS, 30% glycerol, 0.002% bromophenol blue) containing 25 mg/ml DTT for 15 min, followed by equilibration buffer containing 60 mg/ml iodoacetamide for 15 min with agitation at room temperature. The equilibrated strips were placed onto the top of a 12.5% SDS-PAGE gel on mini VE vertical electrophoresis system [GE Healthcare] with a constant voltage of 120 V until the front dye reached to the bottom of the gels. The 2-DE gels were fixed in fixative solution for 30 min and then visualized by CGB staining solution containing 20% methanol, 10% ammonium sulfate, 2% phosphoric acid, and 0.001% colloidal coomassie blue G250 for overnight. Gel images were scanned using ImageScanner II [GEHealthcare] as. mel file for image analysis. The differential protein spots from each fraction were analyzed using Image Master 2-D Platinum software version 5.0 [GE Healthcare]. For matching and quantitative analysis, the reference gel was used for matching the corresponding protein spots among 2-D gels. The matched protein spots from automatic software matching were then confirmed and edited manually. Matching of protein spots across different gels must be consistently found in all triplicate gels. Background subtraction was performed, and the intensity of each spot was normalized with total intensity. Student T test of $p < 0.05$ was used to analyze the percent intensity volume of all protein spots. Protein spots with a statistical change and at least a 1.5-fold change in expression level were selected.

The candidate protein spots were excised and then subjected to in-gel digestion and mass spectrometry. Protein spots were in-gel digested with trypsin (10 ng/µl trypsin containing 50% acetonitrile in 25 mM ammonium bicarbonate) for 18 h at 37 °C. Digested peptides were extracted with 0.1% formic acid in 50% acetonitrile and lyophilized. The digested peptides were dissolved in 0.1% formic acid and then subjected to nano-liquid chromatography coupled with electrospray ionization tandem mass spectrometry (nanoLC-ESI-MS/MS) for protein identification. Database searches for protein identification were performed using the Mascot search engine (www.matrixscience.com). Protein hits with a significant ion score were listed and reported.

2.4. SDS-PAGE and Western blot analysis

For SDS-PAGE, 20 µg of total protein was resolved in 12.5% SDS-PAGE gel. The gels were then visualized by CGB-staining for overnight. For Western blot analysis, the proteins from the 12.5% SDS-PAGE were transferred to PVDF membrane using a Mini *Trans*-Blot electrophoresis transfer cell [Bio-Rad]. The membranes were equilibrated in Tris-glycine transfer buffer containing 39 mM glycine, 0.04% SDS, 10% methanol, and 48 mM Tris-HCl; pH 8.3. Unstained membranes were prepared for hybridization by incubation with blocking solution [5% skimmed milk in TBS buffer (20 mM Tris-HCl, and 150 mM NaCl; pH

7.4) containing 0.1% Tween 20] at 4 °C overnight to prevent non-specific binding. The membranes were incubated in one of the following primary antibodies, including polyclonal rabbit anti-beta-tubulin, anti-VP28, and anti-*Pm*Rab7 (provided by Centex shrimp), anti-14-3-3, and anti-mitogen activated protein kinase 1 (MAPK1) with different dilution in 5% skimmed milk/0.5% TTBS for overnight at 4 °C with agitation. After three washes with 0.5% TTBS, the membranes was incubated at RT for 1 h with respective secondary antibody conjugated with horseradish peroxidase with 1:10,000 in 5% skimmed milk/0.5% TTBS. Immuno-reactive protein bands were visualized with SuperSignal West Pico Chemiluminescent substrate [Pierce]. Blots were scanned by using an Image Scanner II and the relative expression ratio was calculated.

2.5. DNA extraction

Hemocytes were mixed with DNA extraction buffer (100 mM, NaCl, 10 mM Tris-Cl, pH 8.0, 2.5 mM EDTA, 0.5% N-lauroylsarcosine). The reaction were incubated with 0.5 mg/ml RNase A for 30 min at 37 °C followed by 0.5 mg/ml proteinase K for 1 h 56 min at 37 °C. The reactions were mixed with 1% cetyltrimethyl ammonium bromide (CTAB) and incubated for 10 min at 65 °C. Phenol: chloroform (1:1) extraction was performed twice with centrifugation at 15,000*g* for 5 min. DNA was precipitated from aqueous phase by equal volume of isopropanol with −20 °C incubation for 30 min followed by centrifugation at 15,000*g* for 20 min at 4 °C. After air dry, the DNA pellet was rinsed with 70% ethanol and centrifuged at 15,000*g* for 5 min at 4 °C. DNA was dissolved in TE buffer and kept at −20 °C until used.

2.6. PCR and semi quantitative RT-PCR

For PCR detection of WSSV, the total DNA from control and WSSV challenged crabs were mixed with PCR premixed solution (1x PCR buffer, 3 mM $MgCl_2$, 0.2 mM dNTP, 0.5 µM forward and reverse primers, 0.125 U *Taq* DNA polymerase, 100 ng DNA template) with primers specific to wssv419-like protein gene (Table 1). The PCR process were denaturing at 95 °C for 5 min; 25 cycles of 95 °C for 30 s, 55 °C for 30 s, 72 °C for 45 s; final extension at 72 °C for 5 min. The internal control gene was mitochondrial DNA 16S ribosomal RNA gene (Table 1). The PCR products were resolved by 2% agarose gel electrophoresis.

For Reverse transcription PCR (RT-PCR), total RNA was extracted from a pool of hemocyte pellets followed by Trizol® reagent method [Invitrogen]. The first-strand cDNA was prepared from total RNA with Oligo dT_{15} primer. Briefly, the total RNA (1–5 µg) was mixed with 10 µM Oligo dT_{15} primers. The RNA mixture was heated at 65 °C for 5 min. The annealing of primer to RNA template was performed at 25 °C for 10 min and then cooled immediately on ice. Thereafter, the reactions were mixed with 1x reaction buffer containing 2 µl of 10 mM dNTP, 1 U of RevertAid Reverse Transcriptase [Thermo scientific], and RNase-free water. The first-strand cDNA was then used as the template for PCR amplification with the appropriate primers (Table 1). Semi-quantitative RT-PCR analysis was performed on total RNA isolated from control and WSSV infected crab hemocytes. RT-PCR of triose phosphate isomerase (TPI) was performed and used as internal control and for normalization of total RNA variation. RNA expression level was quantitatively analyzed using Image Master 2D Platinum software [GE healthcare].

2.7. Apoptotic assay

An investigation of apoptotic activity was performed in WSSV infected hemocytes using DNA fragmentation and nuclear condensation approaches. For DNA fragmentation method, mud crabs were injected with WSSV (10^5 copies/g) and their hemolymph were obtained at 0, 6, 12, 18, 24, 36, 48, 60, and 72 h post infection (hpi). The hemocytes were isolated by Percoll™ [GE Healthcare] gradient centrifugation. Percoll™ density gradient centrifugation was performed for an isolation of crab hemocyte cell types [16]. The hemolymph was loaded onto the top of 60% Percoll™ gradient (60% Percoll, 0.45 M NaCl) and separated by centrifugation at 2900*g* for 30 min at 4 °C. After centrifugation, separated bands of each hemocyte was observed and aspirated into the new tube. Each hemocyte cell types were collected by centrifugation at 1,900*g* for 2 min at 4 °C. The cells were rinsed about 2–3 times with AC-1 solution and then centrifuged to collect the washed hemocyte pellet. DNAs were extracted from the isolated hemocyte cell types at each time-point. Equal amount of 2 µg DNA was analyzed by 1% agarose gel electrophoresis. The gels were stained by ethidium bromide. The DNA bands were observed under UV transilluminator. Another study to observe nuclear fragmentation of WSSV infected hemocytes was conducted by fluorescent microscopy. Each hemocyte cell types were cultured in L-15 media [Gibco] with 20% fetal bovine serum (FBS) for 1 h and fixed in 4% formaldehyde for 10 min. The hemocytes were mounted on top of Prolong®Gold antifade reagent [Invitrogen] containing DAPI fluorescent dye. DAPI dye will penetrate into nucleus and stained the DNA. The fragmented nucleus revealed the dense fragmented staining of blue DAPI under fluorescent microscope.

2.8. Immunocytochemistry analysis of WSSV-hemocytes interaction

The crabs were injected with WSSV at a fixed dose of 10^5copies/g. After 3 dpi, each hemocyte cell types were isolated and collected by Percoll™ gradient centrifugation as previously mentioned. The fixed hemocytes were permeabilized by 0.1% triton X-100 in PBS buffer, pH 7.4 for 5 min. The hemocytes were rinsed with PBS three times for 5 min each and blocked with 10% FBS in PBS at room temperature for

Table 1
Primers used in PCR and semi-quantitative RT-PCR analysis.

Genes	NCBI Acc. No.	Primer Name	Sequences (5′-3′)	$T_{m\ (°C)}$
wssv419-like protein gene	AY850066	WSSV419_F	atgagaatgaactccaactttaa	48.1
		WSSV419_R	cagagcctagtctatcaatcat	51.1
Mitochondrial DNA 16S ribosomal RNA gene	AF109318	16sar_L	cgcctgtttatcaaaaacat	45.6
	AF109319	16sar_R	ggtctgaactcagatcacgt	51.8
	AF109320			
	AF109321			
Triose phosphate isomerase (TPI)	FJ774782	TPI_F	ggacaacgctatggacagggc	58.3
		TPI_R	gccctctccaagtcagcctcaac	60.6
Translationally-controlled tumor suppressor protein (TCTP)	ACY66461	TCTP_F	cgggatccatgaaggtcttcaag	57.1
		TCTP_R	gcgtcgacttatagcttctcctcg	59.1
C-type lectin (CLEC)	AEI88107	CLEC_F	ttgaatcacaggatgccaga	49.7
		CLEC_R	ctccattaagcggccataac	51.8
Anti-lipopolysaccharide factor 2 (ALPS2)	ADT71676	ALPS2_F	ggacagaagaaacattgaggacgacgca	61.4
		ALPS2_R	ggaaatcaaaaacatccattacaggtca	55.5

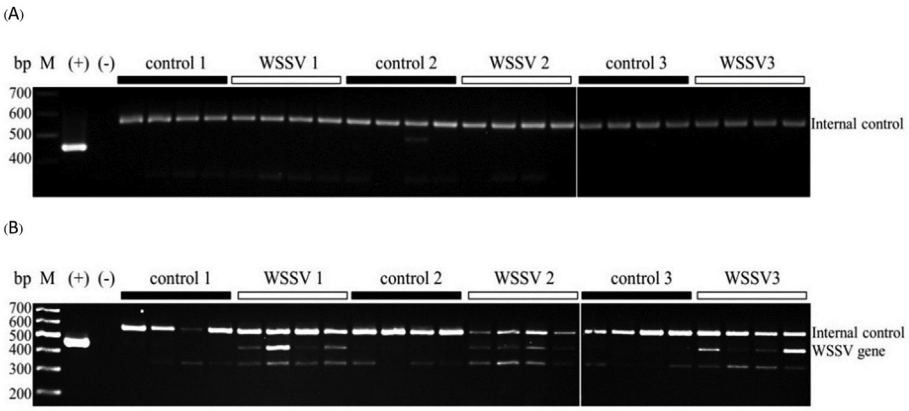

Fig. 1. WSSV screening by PCR. (A) Before WSSV infection, crabs were screened for WSSV infection. The positive band of WSSV419-like protein gene at 446 bps was not observed in all crabs. The mitochondrial 16s rRNA was used as an internal control at 556 bps. (B) After 1 dpi, the control and infected crabs were monitored again by PCR. The expected positive bands of WSSV gene at 446 bps were found only in WSSV-infected group.

1 h. They were incubated with 1:500 rabbit anti-VP28 in 1% FBS/PBS for 1 h at 37 °C. The reactions were rinsed with PBST (PBS, pH7.4 containing 0.001% tween 20) three times for 5 min each. The hemocytes were incubated with 1:500 goat anti-rabbit IgG conjugated with Alexaflor546 in 1%FBS/PBS at room temperature for 1 h. The hemocytes were mounted on top of Prolong®Gold antifade reagent [Invitrogen] containing DAPI fluorescent dye. The signal of WSSV and nucleus was presented in red and blue signal of Alexaflor546 and DAPI fluorescent dye, respectively under confocal fluorescent microscope.

3. Results

3.1. WSSV infection in S. olivacea mud crab

All obtained crabs in the experiment were initially screened for WSSV infection by PCR amplification. The PCR reactions used specific primers encoding for WSSV419-like protein with an internal control primer for mitochondrial 16s rRNA gene. The screening result confirmed that all mud crabs are free from WSSV. These WSSV-free samples gave no positive band corresponding to WSSV gene at 446 bps (Fig. 1). The crabs were then separated into two groups of 12 individual crabs for control and for WSSV infected groups. After an artificial infection of WSSV at the persistent dose of 10^5copies/g, the total hemocyte collected from both groups at 1 day post infection (dpi) were examined by RT-PCR. The results showed the expected 446-bps mRNA bands corresponding to WSSV419-like protein only in the infected group.

3.2. Analysis of differential proteins expression in WSSV-infected hemocytes

The extracted hemocytic proteins obtained from the pooled samples of four individual crabs were fractionated into four fractions by differential centrifugation. Distinctive purity of protein fractions was verified by Western blot analysis using anti-Rab7 antibody. Previous study of Rab7 by ultra-high speed centrifugation showed the presence of Rab7 in hemocyte membrane [46]. Our western blot data showed an immuno-reactive band for Rab7 only in the 20,200*g* fraction (Fig. 2). The result suggested a discriminated purity among these fractions. Each protein fraction from both control and WSSV infected crabs were precipitated and then subjected to 2-D PAGE analysis.

An analysis of each protein fraction was performed on three replicated gels of four crabs each. This experiment therefore represented twelve crabs for control and twelve crabs for WSSV infected groups. That is a total of 24 crabs were used for each 2-D PAGE analysis. Separation of hemocytic protein fractions revealed the 2-D protein spots patterns for control and infected groups in Fig. 3. These 2-D gels corresponding to various fractions gave different protein patterns. Comparative analysis of protein spots between the control and infected groups displayed a numbers of differential proteins.

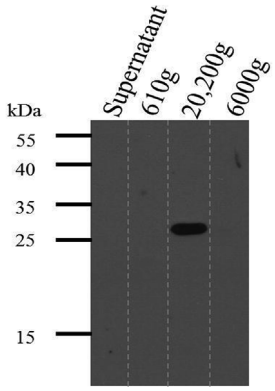

Fig. 2. Validation of purity of fractionated proteins by Western blot analysis for Rab7 Protein. The proteins fractions were resolved by SDS-PAGE and transferred onto PVDF membrane. The immuno-reactive band of Rab7 protein was detected only in the fraction of 20,200*g* centrifugation.

Image analysis revealed a total of 36 differential proteins between the control and WSSV infected proteomes. Differential proteins (>1.5-fold or < 0.67-fold difference) were selected, excised from gels and identified by LC/MS/MS. Database search on MASCOT server successfully identified 36 forms of 31 proteins as summarized in Table 2. Bioinformatics search for molecular function and subcellular localization of these proteins on UniProtKB database and Euk-mPloc protein localization search engine was then conducted. The majority of these proteins (13 out of 31) were suggested for ATP binding activity, while 4 out of 31 proteins were predicted for GTP binding activity. Many other unique and specific molecular functions of identified proteins are listed in Table 2. Subcellular localization for most of the differential proteins (14 out of 31) was in cytoplasm while other protein (7 out of 31) was in the nucleus. Some other proteins such as guanine nucleotide-binding protein G (spot ID 230), Rab-protein 14 (spot ID 708) and vacuolar protein sorting 4B (spot ID 2449) were localized in many cellular compartments. The biological processes related to these 31 proteins were classified into seven groups as shown in Table 2. The altered proteins were also submitted to STRING server (Protein-Protein Interaction Networks) to predict functional associations with other proteins. The result suggested 10 of the total 31 proteins are involved in protein-protein interaction network of four biological processes: (i) anti-apoptosis, (ii) positive regulation of phosphorylation, (iii) regulation of actin cytoskeleton and (iv) actin dependent endocytosis.

3.3. Validation of proteomic data by Western blot analysis and RT-PCR

Three differential proteins [mitogen-activated protein kinase 1 (MAPK1; spot ID 662), crustin (spot ID 1563)], and 14-3-3 zeta proteins (spot ID 505, 1366) were selected for data validation by Western blot

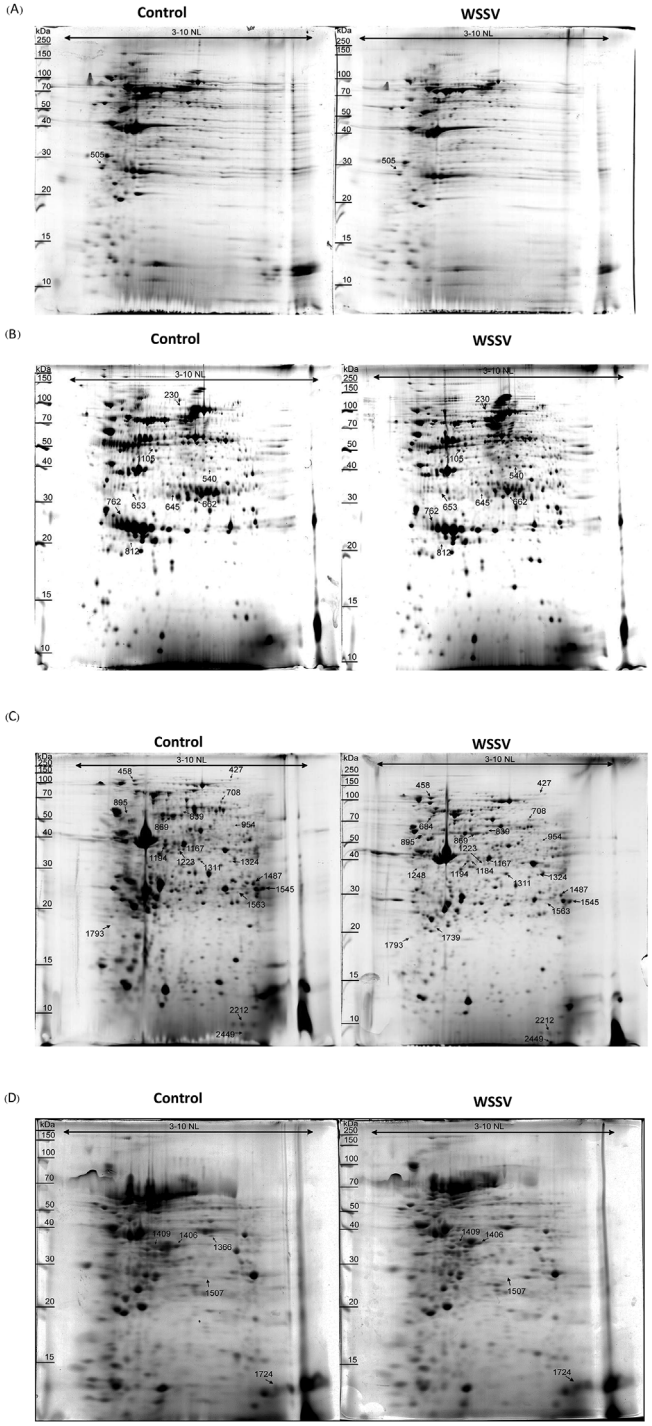

Fig. 3. The representative 2-D gel image of mud crab hemocytes at 1 dpi. The 2-D protein profiles were constructed using 13 cm in-length with 3–10 non-linear IPG strips and 12.5% SDS-PAGE. Each gel contained the pooled protein from three individual crabs. The comparative proteomic was analyzed between control and WSSV-infected. (A) 600*g*, (B) 6,000*g*, (C) 20,200*g* and (D) 20,200*g* supernatant.

analysis. According to the data from 2-D PAGE, an observed % volume of protein spots were increased for MAPK1 and crustin while the spot was decreased for 14-3-3 protein. Western blot analysis was performed by using beta-tubulin as an internal control for normalization. The results clearly confirmed the increased protein abundance of MAPK1 and crustin at approximately 3.0 and 1.6 folds, respectively (Fig. 4). A decrease protein abundance of 14-3-3 zeta in WSSV infected hemocyte was also confirmed at approximately 0.45 fold.

Apart from Western blot analysis, the proteomic data from 2-D gel was also validated at the mRNA level by RT-PCR. Total RNA from the hemocytes of control and 1 dpi WSSV infected crabs were analyzed using triose phosphate isomerase (TPI) as an internal control. The selected target gene included immune responsive genes: translationally control tumor protein (TCTP: spot ID 653), c-type lectin (CLEC: spot ID 1311), and anti-apoptosis gene: anti-lipopolysaccharide factor 2 (ALPS: spot ID 1724). RT-PCR results confirmed a marked increase of mRNA abundance for CLEC at 2.2-folds. However the mRNA abundance of TCTP and ALPS in infected crab did not showed a significant alteration when compared to control (Fig. 5).

3.4. Interaction of WSSV and S. olivacea hemocytes

The WSSV-infected hemocytes at 3 dpi was isolated and characterized for an interaction with WSSV. Microscopic analysis of the isolated hemocytes showed four distinctive cell types. These cell types were classified according to their granulation size into Hyaline (HC), Small Granular (SGC), mixed granular (MGC) and large granular (LGC) cells [30]. Immunofluorescent analysis of these hemocytes, using antibody against WSSV envelope protein (VP28) revealed specific interaction of WSSV particles with small granular (SGC) and large granular cells (LGC) (Fig. 6A). The signal for viral particle (red color) in SGC was observed much higher than that in the LGC. In contrast WSSV signal was not found in mixed granular (MGC) and hyaline cells (HC).

DAPI fluorescent dye staining (blue color) was then applied to elucidate WSSV VP28 localization within the hemocyte cells. WSSV was found co-localized in the cytoplasm and nucleus of the infected SGC, and found only in the nucleus of the infected LGC. Analysis of WSSV-hemocyte interaction was confirmed by Western blot analysis using anti-VP28 antibody. The results also showed an abundance of WSSV in SGC much more than LGC and demonstrated non-detectable level in HC and MGC (Fig. 6B).

3.5. Analysis of WSSV induced apoptosis in S. olivacea hemocytes

The extracted DNA samples from WSSV-infected hemocytes were investigated for apoptotic activity at 0, 6, 12, 18, 24, 36, 48, 60 and 72 hpi. The apoptotic DNA ladders were observed after 60 hpi in HC, SGC MGC and total hemocytes (Fig. 7A). In contrast the ladders were not detected in the LGC and non-infected control group. These hemocyte cells were confirmed for WSSV infectivity by PCR. All WSSV-infected cell types showed the positive band of WSSV419-like protein genes at 446 bps (Fig. 7B). In addition, DAPI fluorescent dye staining was performed to detect nuclear fragmentation. The nuclei were found highly condensed and fragmented in HC, SGC and MGC, except in LGC (Fig. 8). This nuclear condensation result showed good agreement with the data from DNA ladder assay.

4. Discussion

The defense mechanism of mud crab relies on its innate immunity due to a lacking of adaptive immunity. The systemic immune mechanism depends on cellular and humoral immune function of circulating hemocyte and hemolymph, respectively [28]. Previously, four hemocyte cell types of *S. olivacea* were successfully isolated by 60% Percoll™ density gradient centrifugation and characterized [30]. Analysis of LGC indicated the presence of phenoloxidase activity. However, responsive proteins and functional role of other hemocyte cells during WSSV infection remain unknown. In this study, a comparative proteomic analysis and investigation of viral-host interaction of *S. olivacea* hemocytes were implemented aiming to gain an insight for the molecular mechanism WSSV infection in mud crabs.

Proteomic profiles of hemocytes between control and WSSV infected *S. Olivacea* were successfully constructed to reveal differential proteins

Table 2
Differentially expressed proteins in WSSV-infected *S. olivacea* identified by nanoLC-ESI-MS/MS. (*I = found only in WSSV-infected group, C = found only in control group)

Spot ID	Protein [Species]	Accession no.	No. of matched peptides	% cov.	Ion score	pI/Mw (kDa)		Ratio*(WSSV/control)	Function
						Theoretical	Expected		
600 g Fraction									
230	guanine nucleotide-binding protein G(o) subunit alpha 1 [*Daphnia pulex*]	gi|321461127	6	17	259	5.2/41	5.7/90	1.5	Signaling pathway
540	PREDICTED: uridine phosphorylase 1-like [*Apis mellifera*]	gi|66512834	2	5	64	6.0/42	6.1/41	1.76	Metabolism and biosynthesis
645	hemocyanin subunit 1 [*Metacarcinus magister*]	gi|57901139	2	3	89	5.5/67	5.5/34	1.52	Oxygen transport
653	translationally controlled tumor protein [*Scylla paramamosain*]	gi|262401117	3	18	122	4.5/18	4.9/35	1.69	Anti-apoptosis, Immune response
662	mitogen-activated protein kinase 1 [*Meloidogyne artiellia*]	gi|57283051	2	6	62	5.9/46	6.0/33	1.54	Phosphorylation regulation, Signaling pathway
762	DNA repair helicase [*Leifsonia xyli*]	Q6ADK8_LEIXX	2	3	67	5.23/60	4.8/24	0.61	Metabolism and biosynthesis
812	arginine kinase [*Scylla olivacea*]	gi|227955307	4	13	216	6.3/41	4.9/21	0.59	Phosphorylation regulation, Signaling pathway
1105	arginine kinase [*Scylla olivacea*]	gi|227955307	14	46	951	6.3/41	5.2/55	1.52	Phosphorylation regulation, Signaling pathway
6,000 g Fraction									
505	14-3-3 zeta [*Scylla paramamosain*]	gi|380042038	4	23	335	4.8/28	4.6/28	0.48	Phosphorylation regulation, Signaling pathway
20,200 g Fraction									
427	elongation factor-2 [*Libinia emarginata*]	gi|37703953	3	4	153	6.4/82	6.3/117	0.65	Metabolism and biosynthesis
458	tumor rejection antigen (gp96), putative [*Ixodes scapularis*]	gi|241699688	9	10	477	5.0/90	4.9/113	2	Stress response
684	calreticulin precursor [*Fenneropenaeus chinensis*]	gi|84043337	6	14	288	4.3/47	4.8/75	I	Phosphorylation regulation, Signaling pathway
708	Rab-protein 14 [*Danaus plexippus*]	gi|241699689	2	13	131	6.9/24	6.2/70	0.47	Endocytosis and vesicle transport
839	endoplasmin precursor [*Danio rerio*]	gi|38016165	3	4	168	4.7/91	5.6/60	0.64	Anti-apoptosis
869	cortactin, putative [*Pediculus humanus corporis*]	gi|242020140	2	3	91	4.8/46	5.5/55	0.56	Endocytosis and vesicle transport
895	endoplasmin [*Locusta migratoria*]	gi|241997148	3	4	147	4.9/91	4.6/56	2.27	Anti-apoptosis
954	alpha-tubulin [*Eriocheir sinensis*]	gi|330976859	5	17	212	5.0/51	6.4/49	1.73	Metabolism and biosynthesis
1167	chain A, structures of actin-bound Wh2 domins of spire and the implication for filament nucleation [*Oryctolagus cuniculus*]	gi|297343122	6	18	307	5.1/40	5.6/44	1.97	Endocytosis and vesicle transport
1184	heat shock protein 70 [*Scylla paramamosain*]	gi|190589906	16	26	822	5.4/72	5.4/42	I	Stress response
1194	elongation factor-2 [*Eriocheir sinensis*]	gi|384255136	15	18	685	6.3/96	5.4/42	0.55	Metabolism and biosynthesis
1223	beta-actin [*Litopenaeus vannamei*]	gi|10304437	9	28	503	5.3/42	5.6/40	0.22	Metabolism and biosynthesis
1248	actin [*Drosophila melanogaster*]	gi|156773	3	11	131	5.2/42	4.3/40	I	Metabolism and biosynthesis
1311	C-type lectin, partial [*Scylla paramamosain*]	gi|156774	2	24	96	6.0/8.3	5.9/38	2.31	Immune response
1324	glycoprotein 93 [*Drosophila melanogaster*]	gi|21357739	2	2	77	4.9/90	6.3/37	1.57	Stress response
1487	nucleoside permease NupC [*Salmonella enterica*]	gi|145219965	2	4	70	7.8/43	6.9/31	0.66	Metabolism and biosynthesis
1545	cryptocyanin [*Metacarcinus magister*]	gi|4191390	9	14	378	5.5/76	7.5/30	1.57	Oxygen transport
1563	crustin [*Scylla serrata*]	gi|320117470	3	23	157	8.7/13	6.5/29	1.9	Immune response
1739	arginine kinase [*Scylla olivacea*]	gi|227955307	4	14	136	6.3/41	4.9/23	I	Phosphorylation regulation, Signaling pathway
1793	glyceraldehyde-3-phosphate dehyrogenase [*Portunus trituberculatus*]	gi|217795253	3	15	159	6.6/36	4.2/21	1.92	Metabolism and biosynthesis
2212	ubiquitin [*Nematocida parisii ERTm3*]	gi|387592579	4	39	159	10.1/15	6.6/10	1.63	Anti-apoptosis
2449	vacuolar protein sorting 4B [*Scylla paramamosain*]	gi|262401105	2	18	89	9.5/12	6.7/9	2.94	Endocytosis and vesicle transport
Supernatant									
1366	14-3-3 protein [*Scylla paramamosain*]	gi|380003174	10	48	548	4.8/28	6.1/38	C	Phosphorylation regulation, Signaling pathway
1406	vacuolar ATP synthase subunit B K form [*Carcinus maenas*]	gi|6425061	11	28	508	5.3/55	5.6/35	0.46	Metabolism and biosynthesis
1409	beta-actin [*Litopenaeus vannamei*]	gi|10304437	6	25	315	5.3/42	5.3/35	1.67	Endocytosis and vesicle transport
1724	antilipopolysaccharide factor 2 [*Scylla paramamosain*]	gi|91083253	7	52	384	7.8/13	7.5/13	9.01	Immune response
1507	hemocyanin subunit 1 [*Metacarcinus magister*]	gi|57901139	2	3	69	5.5/76	6.1/26	1.67	Oxygen transport

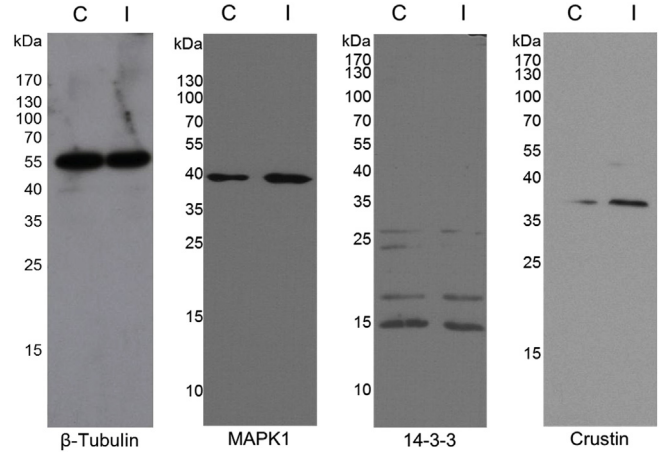

Fig. 4. Western blot analysis of differential proteins response to WSSV infection. Western blot analysis of mitogen-activated protein kinase (MAPK1), 14-3-3 protein and crustin compared between control (C) and 1 dpi of WSSV in crab hemocyte (I). Beta-tubulin was used as an internal control for quantitative normalization. The abundance of MAPK1 and crustin protein was increased and that of 14-3-3 was decreased when compared to the control group.

upon infection. PCR amplification was initially performed to screen for WSSV-free sample and to confirm a success in WSSV infectivity. Prior to proteomic analysis on 2-D PAGE, the complexity of hemocytic proteins were systematically reduced by differential centrifugation. Analyses of all four separated protein fractions gave us a simplified pattern of protein spots, and help increase a coverage of differential proteins. The purity of proteins in each fraction was assessed by Western blot using anti-Rab7. This protein was previously characterized by ultra-centrifugation and found only in the membrane fraction of *P. monodon* [46]. The immuno-reactive band detection of Rab7 revealed good purity of protein fractionation. Image analysis on the 2-D gels of all four fractions revealed a total of 2048 protein spots, with 36 differential protein spots. After a success in protein identification by LC/MS/MS these 36 differential proteins were classified according to biological function into seven groups in (i) immune mechanism, (ii) apoptosis regulation, (iii) endocytosis, (iv) signaling pathway, (v) stress response, (vi) oxygen transport and molting, and (vii) metabolism and bio-synthesis. Validation of our 2-D PAGE data demonstrated good agreement between Western blot analysis results and the observed % volume

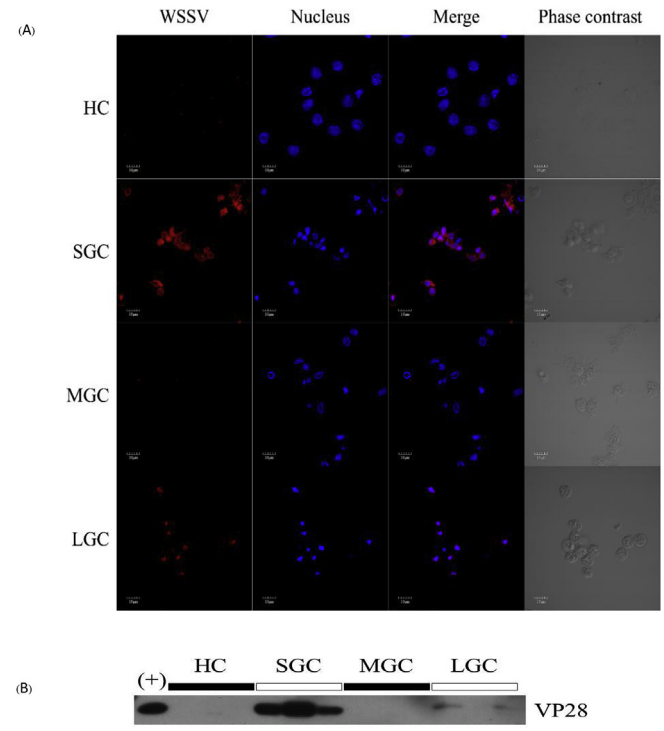

Fig. 6. Immunofluorescence detection of VP28. (A) The interaction of WSSV particles with each hemocyte cell type at 3 dpi were investigated by immunofluorescent staining. WSSV particles were detected in cytoplasmic and nuclear region of SGC and in the nuclear region of LGC. VP28 of WSSV particle was stained in red signal whereas the cell nuclei of was blue signal. Scale bar was 10 μm. (B) Western blot analysis using antibody against VP28 confirmed the immunofluorescence data. (For interpretation of the references to color in this figure legend, the reader is referred to the Web version of this article.)

changes of protein spots on the 2-D gels. All three selected proteins (MAPK1, crustin and 14-3-3) showed similar trends of alteration on both 2-D gels and Western blot membrane. Anti-lipopolysaccharide factor (ALPS) and c-type lectin (CLEC) are immune responsive proteins. They were observed on 2-D gels with the most increased in their protein abundance after WSSV infection. These two proteins were investigated further on their mRNA levels. It is interesting that an increased abundance of CLEC protein was correlated well with the transcription of

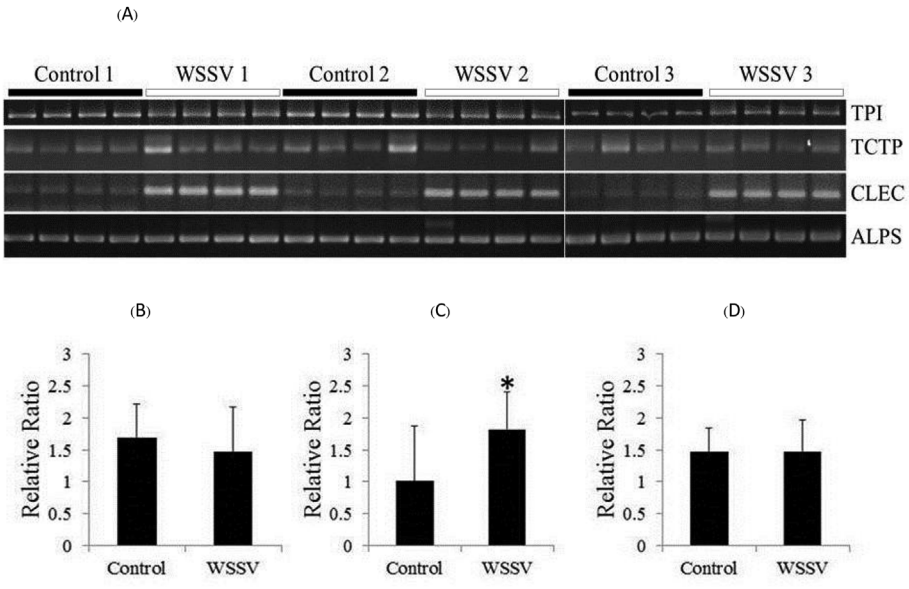

Fig. 5. Semi-quantitative RT-PCR of immune response genes. (A) RT-PCR product of immune response genes: translationally control tumor protein (TCTP), c-type lectin (CLEC), antilipopolysaccharide factor 2 (ALPS), using triose phosphate isomerase (TPI) as internal control to quantitative normalization. (B) TCTP and (D) ALPS transcripts showed no difference between control and WSSV-infected crabs at 1 dpi (p value > 0.05). (C) WSSV-infected CLEC transcripts showed significant difference from the control (p value < 0.05).

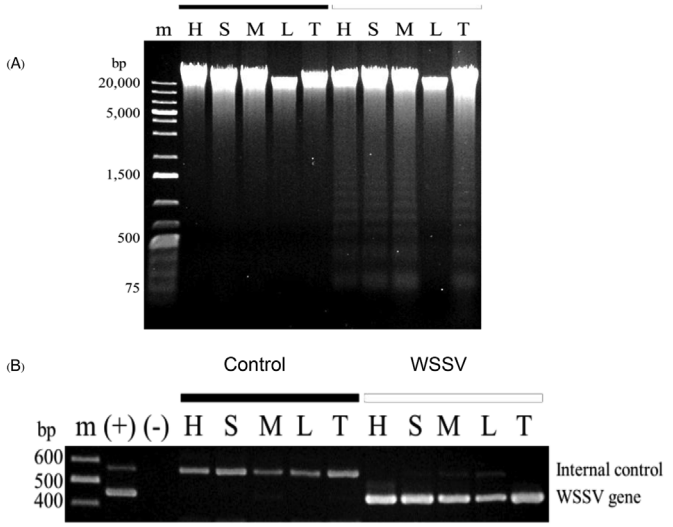

Fig. 7. DNA fragmentation analysis of WSSV infected hemocytes at 60 hpi. (A) Apoptotic ladders of isolated hemocyte cell types from control and WSSV-infected crabs were analyzed by 1% agarose gel electrophoresis. The ladder was appeared in hyaline cells (H), small granular cells (S), mixed granular cells (M), and total hemocytes (T) in WSSV-infected crabs. Meanwhile, large granular cells (L) and control group did not show apoptotic ladder. (B) WSSV infectivity was showed by PCR. The expected positive band of wssv419-like proteins genes at 446 bps was appeared in all infected cell type. The mitochondrial 16s ribosomal RNA gene was used as internal control at l 556 bps.

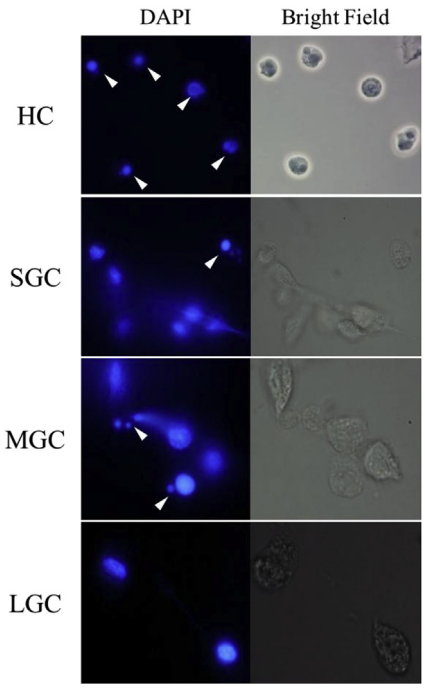

Fig. 8. Nuclear fragmentation analysis of WSSV infected hemocytes. The nuclei of WSSV infected hemocytes were stained by DAPI fluorescent dye (showed as blue signal). The fragmented nuclei were appeared as small dense grain of blue signal (as showed by white arrow) in HC, SGC and MGC whereas no observation of the fragmented nucleus in LGC. (For interpretation of the references to color in this figure legend, the reader is referred to the Web version of this article.)

CLEC gene. In contrast the transcription of ALPS did not change significantly when compared to its increase in protein production. This result confers the transcriptional control regulation of CLEC at the mRNA production, and translational control regulation of ALPS at the protein production after an infection by WSSV.

Among these differential proteins, ALPS and crustin-III were reported to involve with anti-white spot syndrome virus peptides. They were found to be up-regulated in the hemocytes of WSSV-infected *P. monodon* [1]. Moreover, crustin*Pm*1 was also found as a responsive protein involving in shrimp defense mechanism against yellow head virus (YHV) [13]. ALPS has a strong antimicrobial activity. WSSV-challenged freshwater crayfish *P. leniusculus* and prawn *M. rosenbergii* showed up-regulation of the ALPS gene. A knock down pf ALPS by RNAi can lead to a higher level of WSSV propagation, suggesting a crucial role of ALPS as a regulator of WSSV replication [38]. Proteomic study of WSSV-infected *S. paramamosain* hemocyte showed a down-regulation of ALF isoform 5. However this gene showed a trend of up-regulation at 24 hpi. The knockdown of ALPS gene also led to an increase in mortality rate and a decrease in infection time in WSSV-infected crabs [47]. C-type lectin mediated the immune mechanism by recognizing the pathogen and involving in cell-cell interaction [57]. Two c-type lectins were up-regulated in WSSV infected *M. japonicas* and identified as LdlrLec1 and LdlrLec2. These two genes may bind to VP28 and inhibit viral replication in shrimps [61]. An increase of these immune responsive proteins revealed the major role of hemocytes as a defensive tissue for WSSV infection. The study also found an alteration of many proteins relating crucial for an endocytic pathway. The interaction between VP26 and actin may aid endocytosis and promote the internalization of nucleocapsid into the nucleus after the envelop shading [27,60]. Chain A structures of actin-bound Wh2 domains of spire and the implication for filament nucleation protein or Wiskott-Aldrich syndrome effector protein (WAS) was up-regulated upon WSSV infection in this study. During an infection, WAS protein with the role in the nucleation of G-actin to form the filamentous-actin may be important for the actin polymerization [10]. The finding of proteins involved in WSSV entry, especially in endocytosis pathway, may link to membrane protrusion of phagocytosis or micropinocytosis [32]. Vacuolar ATP synthase and vacuolar protein sorting were reported in viral entry via endocytosis of successive infection [37]. Previous study found the binding of VP28 and Rab7, late endosome marker, and suggested the virus entry by endocytosis [46]. Herein, our finding of Rab 14 protein could support the hypothesis of WSSV entry by endocytosis.

Another group of the altered proteins was phosphorylation regulation and signaling pathway proteins. Arginine kinase (AK), a phosphagen enzyme family, was found up-regulated in IHHNV-infected *M. rosenbergii* and WSSV-infected *F. chinensis* in the transcriptional level [2,52]. In this study, the alteration of AK protein also responded to WSSV infection. The previous analysis of WSSV-infected hemolymph of *S. serrata* [29], *V. harveyi*-infected hemocyte of *P. monodon* [44] and YHV-infected gill of *P. vannamei* [36] revealed the increase of AK expression level. Mitogen activated protein kinase 1 (MAPK1) involved in cascading pathway regulates cellular processes such as proliferation, differentiation and cell cycle progression [31]. Our study showed the decreased of MAPK1 substrate, cortactin. This implies that cortactin was phosphorylated by MAPK1 to enhance actin branching and polymerization activity [9]. The up-regulation of MAPK1 may be important for the activation of WSSV entry and viral gene expression in mud crab hemocytes. In signaling pathway, 14-3-3 protein has an ability to prevent the phosphorylation of targeted proteins resulting in both signal amplification and sensitization [19]. Many proteomic analyses of WSSV infection in various crustacean tissues showed an up-regulation of 14-3-3 protein in stomachs of *L. vannamei* [53] and the hepatopancrease of *F. chinensis* [6]. However, 14-3-3 protein was found down-regulated in this experiment. Moreover G-protein complexes, the signal transducers between ligand molecules and cellular processes [33] was increased for subunit α1 upon WSSV infection. It was suggested that the virus infection turn on the signal transduction pathway and downstream cellular processes. Cryptocyanine and hemocyanin subunit 1 were increased in WSSV-infected hemocytes. These two proteins were almost identical. However the phenoloxidase activity was detected only in

hemocyanin [21]. The known function of hemocyanin is also for agglutination activity for bacterial infection [62], antiviral activity [22,65] and antibacterial activity [20]. Other identified proteins were general metabolic and physiological responsive proteins.

Our study on the interaction between various hemocyte cells of *S. olivacea* and WSSV showed different level of viral susceptibility (Fig. 8B). The results from immunofluorescent detection revealed that SGC is more susceptible to WSSV than LGC while HC and MGC showed much lower infection. The virus replication was observed in all types of hemocyte cells. However the assembly of WSSV proteins into virion was detected only in SGC and LGC. The difference in susceptible level of crustacean hemocyte cell types to viral infection was commonly reported. In crayfish and *Penaeus merguiensis*, Semi-granular cells were found more susceptible to WSSV than granular cells [17,55]. Our recent data also demonstrated interaction and replication of yellow head virus mainly with the granule-containing hemocytes (SGC and GC) and little to none in HC [13]. In this study WSSV induced apoptosis of crab hemocytes was clearly detected at 60 hpi in HC, SGC and MGC but not in LGC. It is common to observe WSSV induced apoptosis in the hemocytes of *Penaeus monodon*, *Penaeus indicus* [41] and *Penaeus liniusculus* shrimps [17]. The induction of hemocyte apoptosis by WSSV infection was also found on specific cell types. Our findings suggest that mud crab may encounter WSSV infection and replication by inducing of apoptosis. An escape or delay of apoptosis could be used by viruses as the mechanism for their success in replication. Some viruses take an advantage of apoptosis as a tool for cell killing and spreading of virions [40].

The molecular mechanism of WSSV-induced apoptosis in host cell and WSSV regulation were investigated [25]. When the WSSV infection initiates, cellular sensors detect and activate the signaling pathway to induce the expression of apoptosis regulating proteins. The proteins such as *Pm*Casp (an effecter caspase), MjCaspase (an initiator caspase) and voltage-dependent anion channel (VDAC) [26,54,58] were found together with an increased oxidative stress to initiate the apoptosis program. Meanwhile, to prevent apoptosis and replication, WSSV starts to express anti-apoptosis proteins such as AAP-1 (WSSV449) and WSSV222. AAP-1, a direct caspase inhibitor, functions at the apoptotic regulating point by blocking the activity of caspase 3 protein [23,56]. WSSV222 blocks apoptosis through the ubiquitin-mediated proteolysis of shrimp tumor suppressor-like protein (an apoptosis inducer) to accomplish successful replication in *Penaeus vannamei* [14]. WSSV was reported to induces shrimp anti-apoptosis proteins such as translationally control tumor protein, inhibitor of apoptosis protein (IAP) and *Pm*-fortilin in *P. monodon* [18,24]. When replication and virion assembly were achieved at a favorable level, WSSV may release apoptosis inducing proteins or induce an expression of host apoptosis proteins. The infected cells then undergo apoptosis and release the complete virion [25]. This phenomenon leads to cell death in the infected host cells. In this work, we found an increase of TCTP protein abundance (TCTP; spot ID 653) while the mRNA level was not changed significantly. The result confers a translational control regulation of this TCTP during WSSV infection. TCTP or fortilin has biological functions in anti-apoptosis, response to virus and stem cell maintenance. In *P. monodon* shrimp, TCTP was up-regulated at an early phase of WSSV infection, the expression level was reduced at moribund stage [4,11]. The shrimp TCTP transfected into human osteosarcoma cell line (U2OS cell) was also reported for anti-apoptosis assay. The results showed the ability of TCTP to protect the human cell line from death under toxic condition [11]. Moreover, the overexpression of shrimp TCTP in sf9 cell can inhibit the expression of early gene (*WSSV-DNA polymerase*) and late gene (*VP15* and *VP28*) of WSSV but not immediate early gene (ie1) ([34]. Moreover a recombinant TCTP was found capable to inhibit WSSV infection leading to 80–100% survival for infected shrimp [48].

The difference in WSSV susceptibility and apoptosis of each mud crab hemocyte cells may imply a specific activity and participation in viral infection. Our PCR study showed WSSV susceptibility in all cell types. However HC and MGC undergo apoptosis to prevent complete assembly of the WSSV virion. In SGC the complete virion was detected together with apoptosis. It is possible that apoptosis was delayed by WSSV to boost viral propagation and maturation to a favorable level before releasing out via apoptosis. It was supported by our previous report that the number of mud crab SGC decreased significantly at late infection period of 4 dpi [30]. In contrast LGC showing WSSV susceptibility and virion formation did not proceed to apoptosis. An inhibition of apoptosis was supported by a slight decrease of LGC observed in infected crab [30]. However, the detailed mechanism of apoptosis inhibition and a possible latent habitat for WSSV in LGC is still unclear and therefore attractive for further investigated.

In conclusion, we have identified differential proteins in *S. olivacea* hemocytes upon WSSV infection. The regulation of some altered proteins was confirmed and investigated in infected cells in both transcription and translation levels. The functional roles of these altered proteins could be related to several host response processes including immune responsive and anti-apoptotic proteins. Moreover all of hemocyte cell types were demonstrated to be infected with different levels of WSSV susceptibility and apoptotic responses. The induced apoptosis by WSSV revealed in HC and MGC, was suggested to be delayed and inhibited in SGC and LGC respectively. The results provide an essential insight for a better understanding of molecular interaction between WSSV and distinctive types of hemocytes. This study could lead to further research and development for control and management of the viral diseases in aquaculture production.

Acknowledgement

This work was supported by the Thailand Research Fund (TRF) and Mahidol University.

References

[1] S.P. Antony, et al., Anti-lipopolysaccharide factor and crustin-III, the anti-white spot virus peptides in *Penaeus monodon*: control of viral infection by up-regulation, Aquaculture 319 (2011) 11–17.
[2] J. Arockiaraj, et al., Gene profiling and characterization of arginine kinase-1 (MrAK-1) from freshwater giant prawn (*Macrobrachium rosenbergii*), Fish Shellfish Immunol. 31 (2011) 81–89.
[3] W. Assavalapsakul, D.R. Smith, S. Panyim, Identification and characterization of a *Penaeus monodon* lymphoid cell-expressed receptor for the yellow head virus, J. Virol. 80 (2006) 262–269.
[4] P. Bangrak, et al., Molecular cloning and expression of a mammalian homologue of a translationally controlled tumor protein (TCTP) gene from *Penaeus monodon* shrimp, J. Biotechnol. 108 (2004) 219–226.
[5] Y.-M. Chai, et al., Comparative proteomic profiles of the hepatopancreas in *Fenneropenaeus chinensis* response to white spot syndrome virus, Fish Shellfish Immunol. 29 (2010) 480–486.
[6] Y.M. Chai, et al., Comparative proteomic profiles of the hepatopancreas in *Fenneropenaeus chinensis* response to white spot syndrome virus, Fish Shellfish Immunol. 29 (2010) 480–486.
[7] J. Chen, et al., Characterization of a novel envelope protein WSV010 of shrimp white spot syndrome virus and its interaction with a major viral structural protein VP24, Virol 364 (2007) 208–213.
[8] V. Corbel, et al., Experimental infection of European crustaceans with white spot syndrome virus (WSSV), J. Fish Dis. 24 (2001) 377–382.
[9] L.I. Cosen-Binker, A. Kapus, Cortactin: the gray eminence of the cytoskeleton, Physiol. 21 (2006) 352–361.
[10] A.M. Ducka, et al., Structures of actin-bound Wiskott-Aldrich syndrome protein homology 2 (WH2) domains of Spire and the implication for filament nucleation, Proc. Natl. Acad. Sci. U.S.A. 107 (2010) 11757–11762.
[11] P. Graidist, et al., Establishing a role for shrimp fortilin in preventing cell death, Aquaculture 255 (2006) 157–164.
[12] A.S. Hameed, et al., Experimental infection of twenty species of Indian marine crabs with white spot syndrome virus (WSSV), Dis. Aquat. Org. 57 (2003) 157–161.
[13] P.O. Havanapan, et al., Yellow head virus infection in black tiger shrimp reveals specific interaction with granule-containing hemocytes and crustin*Pm*1 as a responsive protein, Dev. Comp. Immunol. 54 (2016) 126–136.
[14] F. He, et al., White spot syndrome virus open reading frame 222 encodes a viral E3 ligase and mediates degradation of a host tumor suppressor via ubiquitination, J. Virol. 80 (2006) 3884–3892.
[15] M.S. Hossain, et al., Detection of white spot syndrome virus (WSSV) in wild captured shrimp and in non-cultured crustaceans from shrimp ponds in Bangladesh by polymerase chain reaction, Fish Pathol. 36 (2001) 93–95.

[16] C. Imjongjirak, et al., Molecular cloning and characterization of crustin from mud crab *Scylla paramamosain*, Mol. Biol. Rep. 36 (2009) 841–850.
[17] P. Jiravanichpaisal, et al., White spot syndrome virus (WSSV) interaction with crayfish haemocytes, Fish Shellfish Immunol. 20 (2006) 718–727.
[18] M.W. Johansson, et al., Crustacean haemocytes and haematopoiesis, Aquaculture 191 (2000) 45–52.
[19] R. Kleppe, et al., The 14-3-3 proteins in regulation of cellular metabolism, Semin. Cell Dev. Biol. 22 (2011) 713–719.
[20] S.Y. Lee, B.L. Lee, K. Soderhall, Processing of an antibacterial peptide from hemocyanin of the freshwater crayfish *Pacifastacus leniusculus*, J. Biol. Chem. 278 (2003) 7927–7933.
[21] S.Y. Lee, B.L. Lee, K. Söderhäll, Processing of crayfish hemocyanin subunits into phenoloxidase, Biochem. Biophys. Res. Commun. 322 (2004) 490–496.
[22] K. Lei, et al., Difference between hemocyanin subunits from shrimp *Penaeus japonicus* in anti-WSSV defense, Dev. Comp. Immunol. 32 (2008) 808–813.
[23] J.H. Leu, et al., Molecular mechanism of the interactions between white spot syndrome virus anti-apoptosis protein AAP-1 (WSSV449) and shrimp effector caspase, Dev. Comp. Immunol. 34 (2010) 1068–1074.
[24] J.H. Leu, et al., Molecular cloning and characterization of an inhibitor of apoptosis protein (IAP) from the tiger shrimp, *Penaeus monodon*, Dev. Comp. Immunol. 32 (2008) 121–133.
[25] J.H. Leu, et al., A model for apoptotic interaction between white spot syndrome virus and shrimp, Fish Shellfish Immunol. 34 (2013) 1011–1017.
[26] J.H. Leu, et al., Penaeus monodon caspase is targeted by a white spot syndrome virus anti-apoptosis protein, Dev. Comp. Immunol. 32 (2008) 476–486.
[27] B. Liu, X. Tang, W. Zhan, Interaction between white spot syndrome virus VP26 and hemocyte membrane of shrimp, *Fenneropenaeus chinensis*, Aquaculture 314 (2011) 13–17.
[28] H. Liu, K. Söderhäll, P. Jiravanichpaisal, Antiviral immunity in crustaceans, Fish Shellfish Immunol. 27 (2009) 79–88.
[29] W. Liu, D. Qian, X. Yan, Proteomic analysis of differentially expressed proteins in hemolymph of *Scylla serrata* response to white spot syndrome virus infection, Aquaculture 314 (2011) 53–57.
[30] S. Mangkalanan, et al., Characterization of the circulating hemocytes in mud crab (*Scylla olivacea*) revealed phenoloxidase activity, Dev. Comp. Immunol. 44 (2014) 116–123.
[31] S. Meloche, J. Pouyssegur, The ERK1/2 mitogen-activated protein kinase pathway as a master regulator of the G1- to S-phase transition, Oncogene 26 (2007) 3227–3239.
[32] J. Mercer, A. Helenius, Virus entry by macropinocytosis, Nat. Cell Biol. 11 (2009) 510–520.
[33] S.R. Neves, P.T. Ram, R. Iyengar, G protein pathways, Science (New York, N.Y.) 296 (2002) 1636–1639.
[34] B. Nupan, et al., Shrimp Pm-fortilin inhibits the expression of early and late genes of white spot syndrome virus (WSSV) in an insect cell method, Dev. Comp. Immunol. 35 (2011) 469–475.
[35] K.V. Rajendran, et al., Experimental host range and histopathology of white spot syndrome virus (WSSV) infection in shrimp, prawns, crabs and lobsters from India, J. Fish Dis. 22 (1999) 183–191.
[36] T. Rattanarojpong, et al., Analysis of differently expressed proteins and transcripts in gills of *Penaeus vannamei* after yellow head virus infection, Proteomics 7 (2007) 3809–3814.
[37] C. Recchi, P. Chavrier, V-ATPase: a potential pH sensor, Nat. Cell Biol. 8 (2006) 107–109.
[38] Q. Ren, et al., Three different anti-lipopolysaccharide factors identified from giant freshwater prawn, *Macrobrachium rosenbergii*, Fish Shellfish Immunol. 33 (2012) 766–774.
[39] P. Roch, Defense mechanisms and disease prevention in farmed marine invertebrates, Aquaculture 172 (1999) 125–145.
[40] A. Roulston, R.C. Marcellus, P.E. Branton, Viruses and apoptosis, Annu. Rev. Microbiol. 53 (1999) 577–628.
[41] A.S. Sahul Hameed, et al., Quantitative assessment of apoptotic hemocytes in white spot syndrome virus (WSSV)-infected penaeid shrimp, *Penaeus monodon* and *Penaeus indicus*, by flow cytometric analysis, Aquaculture 256 (2006) 111–120.
[42] M. Sarathi, et al., Clearance of white spot syndrome virus (WSSV) and immunological changes in experimentally WSSV-injected *Macrobrachium rosenbergii*, Fish Shellfish Immunol. 25 (2008) 222–230.
[43] N. Somboonna, et al., Mud crab susceptibility to disease from white spot syndrome virus is species-dependent, BMC Res. Notes 3 (2010) 315-315.
[44] K. Somboonwiwat, et al., Proteomic analysis of differentially expressed proteins in *Penaeus monodon* hemocytes after *Vibrio harveyi* infection, Proteome Sci. 8 (2010) 39.
[45] J. Srisala, et al., Comparison of white spot syndrome virus PCR-detection methods that use electrophoresis or antibody-mediated lateral flow chromatographic strips to visualize PCR amplicons, J. Virol Methods 153 (2008) 129–133.
[46] K. Sritunyalucksana, et al., PmRab7 is a VP28-binding protein involved in white spot syndrome virus infection in shrimp, J. Virol. 80 (2006) 10734–10742.
[47] B. Sun, et al., A proteomic study of hemocyte proteins from mud crab (*Scylla paramamosain*) infected with white spot syndrome virus or *Vibrio alginolyticus*, Front. Immunol. 8 (2017) 468.
[48] M. Tonganunt, et al., The role of Pm-fortilin in protecting shrimp from white spot syndrome virus (WSSV) infection, Fish Shellfish Immunol. 25 (2008) 633–637.
[49] J.M. Tsai, et al., Genomic and proteomic analysis of thirty-nine structural proteins of shrimp white spot syndrome virus, J. Virol. 78 (2004) 11360–11370.
[50] J.M. Tsai, et al., Identification of the nucleocapsid, tegument, and envelope proteins of the shrimp white spot syndrome virus virion, J. Virol. 80 (2006) 3021–3029.
[51] C.B. van de Braak, et al., Preliminary study on haemocyte response to white spot syndrome virus infection in black tiger shrimp *Penaeus monodon*, Dis. Aquat. Org. 51 (2002) 149–155.
[52] B. Wang, et al., Discovery of the genes in response to white spot syndrome virus (WSSV) infection in *Fenneropenaeus chinensis* through cDNA microarray, Mar. Biotechnol. 8 (2006) 491–500.
[53] H.C. Wang, et al., Protein expression profiling of the shrimp cellular response to white spot syndrome virus infection, Dev. Comp. Immunol. 31 (2007) 672–686.
[54] L. Wang, et al., Requirement for shrimp caspase in apoptosis against virus infection, Dev. Comp. Immunol. 32 (2008) 706–715.
[55] Y.T. Wang, et al., White spot syndrome virus (WSSV) infects specific hemocytes of the shrimp *Penaeus merguiensis*, Dis. Aquat. Org. 52 (2002) 249–259.
[56] Z. Wang, et al., ORF390 of white spot syndrome virus genome is identified as a novel anti-apoptosis gene, Biochem. Biophys. Res. Commun. 325 (2004) 899–907.
[57] W.I. Weis, M.E. Taylor, K. Drickamer, The C-type lectin superfamily in the immune system, Immunol. Rev. 163 (1998) 19–34.
[58] K. Wongprasert, et al., Cloning and characterization of a caspase gene from black tiger shrimp (*Penaeus monodon*)-infected with white spot syndrome virus (WSSV), J. Biotechnol. 131 (2007) 9–19.
[59] J. Wu, et al., White spot syndrome virus proteins and differentially expressed host proteins identified in shrimp epithelium by shotgun proteomics and cleavable isotope-coded affinity tag, J. Virol. 81 (2007) 11681–11689.
[60] X. Xie, F. Yang, Interaction of white spot syndrome virus VP26 protein with actin, Virol 336 (2005) 93–99.
[61] Y.H. Xu, et al., Two novel C-type lectins with a low-density lipoprotein receptor class A domain have antiviral function in the shrimp *Marsupenaeus japonicus*, Dev. Comp. Immunol. 42 (2014) 323–332.
[62] F. Yan, et al., Identification and agglutination properties of hemocyanin from the mud crab (*Scylla serrata*), Fish Shellfish Immunol. 30 (2011) 354–360.
[63] G. Yi, et al., Vp28 of shrimp white spot syndrome virus is involved in the attachment and penetration into shrimp cells, J. Biochem. Mol. Biol. 37 (2004) 726–734.
[64] W. Youtong, et al., WSSV: VP26 binding protein and its biological activity, Fish Shellfish Immunol. 30 (2011) 77–83.
[65] X. Zhang, C. Huang, Q. Qin, Antiviral properties of hemocyanin isolated from shrimp *Penaeus monodon*, Antivir. Res. 61 (2004) 93–99.
[66] Y. Zhou, et al., Hemocytes of the mud crab Scylla paramamosain: cytometric, morphological characterization and involvement in immune responses, Fish Shellfish Immunol. 72 (2018) 459–469.